JOURNAL OF GEOPHYSICAL RESEARCH, VOL. 107, NO. E6, 5039, 10.1029/2001JE001590, 2002

Pyroxene reflectance spectra: Minor absorption bands and effects of elemental substitutions

Edward A. Cloutis

Department of Geography, University of Winnipeg, Winnipeg, Manitoba, Canada

Received 5 September 2001; revised 23 November 2001; accepted 19 December 2001; published 13 June 2002.

[1] Reflectance spectra of a suite of compositionally diverse pyroxenes exhibit variable spectral properties which are associated with various elemental substitutions. Those associated with transition series elements, such as Cr, Ti, V, and Mn, give rise to a number of minor absorption bands in the visible spectral region and, in some cases (e.g., Mn), at longer wavelengths. Substitutions by other cations, such as Li and Zr, do not result in distinct absorption bands. The spectra of these pyroxenes are dominated by the transition series elements that may be present in the samples. The visible wavelength region of low-calcium pyroxene reflectance spectra exhibit a number of absorption bands which are attributable to Fe^{2+} spin-forbidden crystal field transitions. Fe^{2+}-Fe^{3+} intervalence charge transfer absorption bands near 0.77 μm are common in terrestrial pyroxenes which contain both ferrous and ferric iron. Collectively, these results indicate that the presence of various transition series elements can be detected in reflectance spectra and that their oxidation states and site occupancies can also be determined on the basis of unique spectral characteristics present in their reflectance spectra, thereby greatly increasing the range of compositional information which can be derived from analysis of their reflectance spectra. *INDEX TERMS:* 3620 Mineralogy and Petrology: Crystal chemistry; 3670 Mineralogy and Petrology: Minor and trace element composition; 3694 Mineralogy and Petrology: Instruments and techniques; 3934 Mineral Physics: Optical, infrared, and Raman spectroscopy; 6008 Planetology: Comets and Small Bodies: Composition; *KEYWORDS:* pyroxene, reflectance spectroscopy, transition series elements, asteroids

1. Introduction

[2] Pyroxenes are among the most widespread minerals present on the surfaces of inner solar system bodies. They are known or inferred to exist on the surfaces of Mercury [*McCord and Clark*, 1979], Venus [*Surkov et al.*, 1983], the Earth and Moon [*Basaltic Volcanism Study Project*, 1981], Mars [*Wood and Ashwal*, 1981; *Huguenin*, 1987; *Singer et al.*, 1990], and certain classes of asteroids [*McCord et al.*, 1970; *Feierberg et al.*, 1980; *Cruikshank et al.*, 1991] and meteorites [e.g., *Dodd*, 1981]. Their detection on remote surfaces can be accomplished through the analysis of reflectance spectra spanning the range from 0.3 to 2.6 μm, a wavelength range readily amenable to Earth- and space-based observations.

[3] Low-calcium pyroxene (LCP) reflectance spectra in the 0.3–2.6 μm region are characterized by two major absorption bands situated near 0.9 μm (band I) and 1.9 μm (band II) which are of roughly equal intensity and are attributed to crystal field transitions in Fe^{2+} which preferentially occupies the M2 crystallographic site (Figure 1) [e.g., *Clark*, 1957; *Ghose*, 1965; *White and Keester*, 1966; *Bancroft and Burns*, 1967; *Bancroft et al.*, 1967a; *Burns et al.*, 1972a, 1972b; *Roush*, 1984; *Burns*, 1993]. More complex spectra are possible in very iron-rich (>∼50 Fs) LCPs, where iron occupies both M1 and M2 sites [*Ross and Sowerby*, 1996].

[4] High-calcium pyroxene (HCP) spectra can be broadly assigned to one of two types (type A or type B) on the basis of their absorption bands. Type B spectra are superficially similar to LCPs with two major absorption bands near 1.05 μm (band I) and 2.35 μm (band II) (Figure 1). In HCPs, calcium is strongly partitioned into the M2 crystallographic site with Fe^{2+} (and other cations) often making up for any deficiencies in full M2 site occupancy by calcium. The absorption bands in these type B HCP spectra are attributed to Fe^{2+} M2 site crystal field transitions [*Hazen et al.*, 1978; *Rossman*, 1980; *Burns*, 1993]. Type A spectra exhibit two major absorption bands near 0.9 and 1.15 μm (Figure 1). These bands are assigned to Fe^{2+} M1 site crystal field transitions [*Adams*, 1975; *Burns*, 1993]. Type A spectra are almost exclusively confined to HCPs containing >50 mol % Wo [*Cloutis and Gaffey*, 1991]. HCPs with spectra intermediate between these two types are also possible and are indicative of spectral contributions from Fe^{2+} situated in both the M1 and M2 crystallographic sites [*White and Keester*, 1966; *Bell and Mao*, 1972a; *Burns et al.*, 1972b]. Iron-bearing pyroxenes will also exhibit less intense absorption bands in the 0.4–0.8 μm region as described in section 3.9.

[5] The spectral-compositional relationships for pyroxenes have been developed by a number of investigators [e.g., *Adams*, 1974, 1975; *Hazen et al.*, 1978; *Cloutis and Gaffey*, 1991]. In general, the wavelength positions of the

0148-0227/02/2001JE001590

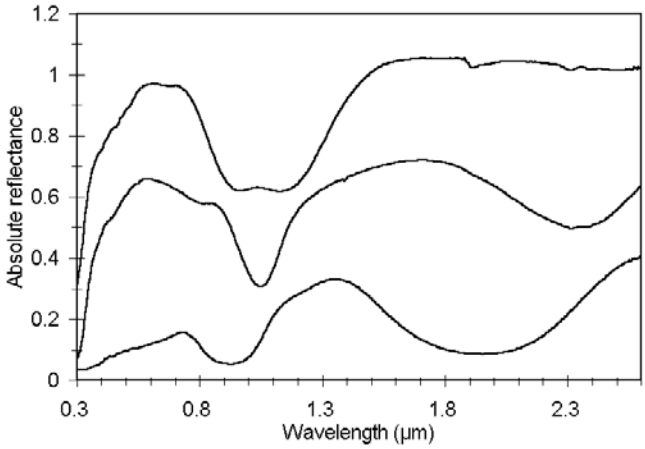

Figure 1. Reflectance spectra of 45–90 μm grain size fractions of "typical" pyroxenes, containing <0.5 wt % of transition series elements: (top) a type A high-calcium pyroxene ($Fs_{10}En_{40}Wo_{50}$; vertically offset by +0.2 for clarity), (middle) a type B high-calcium pyroxene ($Fs_2En_{49}Wo_{49}$), and (bottom) a low-calcium pyroxene ($Fs_{41}En_{55}Wo_4$).

two major Fe^{2+} absorption bands move to longer wavelengths with increasing iron and calcium contents, and band positions can be used to constrain the major cation abundances. A number of investigators have noted that samples containing transition series elements such as Ti and Cr in abundances exceeding ~1 wt % (i.e., >1 wt % TiO_2 or Cr_2O_3) tended to display anomalous reflectance spectra in terms of the wavelength positions of the major absorption bands in the 1 and 2 μm regions which were found to fall off the trend between band position and Fe and Ca contents.

[6] This study was undertaken to address a number of issues including resolving whether Cr- and Ti-bearing pyroxenes exhibit systematic offsets from the spectral-compositional trends determined by *Adams* [1974], *Hazen et al.* [1978], and *Cloutis and Gaffey* [1991], assessing the spectrum-altering effects of various elemental substitutions, and determining the causes of minor absorption bands seen in some pyroxene reflectance spectra. The goal of this study was to gain a more comprehensive understanding of the range of spectral reflectance properties of pyroxene group minerals and to determine whether site occupancies and oxidation states of various transition series elements can be determined from analysis of pyroxene reflectance spectra.

2. Experimental Procedure

[7] A number of naturally occurring terrestrial pyroxenes were included in this study. Their compositions were determined by electron microprobe analysis at the University of Calgary scanning electron microprobe quantometer facility and are an average of from four- to eight-point analyses or area scans. The data were reduced using Bence-Albee α and β correction factors. The Fe^{2+} values were determined by wet-chemical methods [*Hillebrand and Lundell*, 1953], and Fe^{3+} values were determined as the difference between total and ferrous iron. The identities of the samples were also confirmed by X-ray diffraction. Analytical data for the samples are provided in Table 1.

[8] The sample powders used for spectral analysis were prepared by crushing the samples in an alumina mortar and pestle. Accessory phases which were present in some of the samples, consisting largely of opaque minerals such as magnetite and various alteration products, were removed as much as possible through a combination of hand picking and magnetic separation. The cleaned separates were repeatedly wet sieved with acetone to obtain well-sorted size fractions.

[9] The reflectance spectra were measured at the Reflectance Experiment Laboratory (RELAB) spectrometer facility at Brown University [*Pieters*, 1983; *RELAB*, 1996]. The spectra were measured from 0.3 to 2.6 μm at 5 nm spectral resolution. The 45–90 μm fractions of all of the samples, with the exception of PYX 124, 125, 150, 170, 180, and 182, were spectrally characterized; for these other six samples the <45 μm fractions were characterized. All of the sample spectra were measured at $i = 30°$ and $e = 0°$ relative to halon, a near-perfect diffuse reflector in the 0.3 to 2.6 μm region [*Weidner and Hsia*, 1981]. The spectra were also corrected for minor (~2%) irregularities in halon's absolute reflectance in the 2 μm region and dark current offsets.

[10] The wavelength positions of absorption bands were determined by fitting a third-order polynomial equation to between 10 and 20 data points on either side of a visually determined minimum or center. Absorption bands for which no continuum removal was applied are termed band minima. In some cases, absorption bands were isolated by dividing the spectrum by a straight-line continuum tangent to the reflectance spectrum on either side of an absorption feature of interest. The wavelength position of minimum reflectance of features isolated in this way are referred to as band centers.

3. Site Occupancies by Transition Series Elements

[11] The order in which cations are assigned to the various structural sites in pyroxenes is generally as follows: The sites are filled in the order tetrahedral, then M1, then M2; and cations are assigned in the following order: Si, Al, Fe^{3+}, Ti^{4+}, Cr, Mg, Fe^{2+}, Mn, Ca, then Na. In LCPs, ferrous iron preferentially occupies the M2 crystallographic site, while in HCPs, Ca is strongly partitioned into the M2 site, with ferrous iron (and other cations) making up any deficiencies in Ca M2 site occupancy [*Warren and Bragg*, 1929; *Clark*, 1957; *Ghose*, 1965; *White and Keester*, 1966; *Bancroft and Burns*, 1967; *Bancroft et al.*, 1967a; *Burns*, 1970; *Burns et al.*, 1972a, 1972b].

[12] A number of studies have demonstrated that Na, Co^{2+}, Zn^{2+}, Cr^{2+}, and Mn^{2+} preferentially occupy the larger and more distorted M2 crystallographic site in orthopyroxenes, pigeonites, and clinopyroxenes [*Angel et al.*, 1989; *Bancroft et al.*, 1967a, 1967b; *Cameron and Papike*, 1980; *Davoli et al.*, 1987; *Burns*, 1993], while trivalent cations, such as Cr^{3+}, Al^{3+}, V^{3+}, Fe^{3+}, Ti^{3+}, as well as Ti^{4+} and Ni^{2+}, preferentially occupy the M1 site [*Tazzoli and Domeneghetti*, 1987; *Molin*, 1989; *Burns*, 1993]. A comprehensive study of LCPs [*Howie and Smith*, 1966] suggests that Mn content is positively correlated with Fe content, while Ni and Cr contents are negatively correlated with Fe content. The M1 site in HCPs is preferentially occupied by Fe^{3+},

Table 1. Compositions of Pyroxenes Used in This Study[a]

	PYX 013	PYX 018	PYX 019	PYX 023	PYX 029	PYX 033	PYX 035	PYX 040	PYX 042	PYX 044
SiO_2	52.48	55.17	48.41	56.86	51.56	48.46	48.05	47.27	56.59	47.25
Al_2O_3	0.56	0.37	5.29	0.76	3.48	1.01	5.15	8.28	0.09	<0.01
FeO	0.50	2.42	6.15	6.36	4.20	6.02	6.29	4.69	8.93	0.13
Fe_2O_3	14.55	0.00	3.79	0.83	1.39	7.73	2.56	2.77	0.84	0.00
MgO	8.05	17.01	12.37	34.04	14.01	3.54	13.12	13.19	33.88	2.44
CaO	13.14	23.93	22.15	0.65	24.22	17.65	21.95	20.90	0.22	5.95
Na_2O	5.91	0.51	0.36	0.00	0.40	2.59	0.53	0.63	0.00	0.03
TiO_2	0.01	<0.01	1.05	0.01	0.38	0.02	1.73	1.73	0.04	<0.01
Cr_2O_3	0.04	0.91	0.03	0.45	0.03	0.06	0.03	0.43	0.04	0.08
V_2O_5	0.01	0.03	0.03	<0.01	0.00	0.00	0.02	<0.01	<0.01	0.01
CoO	0.05	0.02	0.05	0.03	0.03	0.06	0.04	0.03	0.02	0.09
NiO	0.02	0.07	0.02	0.08	0.03	0.06	0.02	0.03	0.01	0.12
MnO	5.17	0.10	0.26	0.17	0.31	7.66	0.19	0.11	0.04	42.81
ZrO_2	0.00	0.00	0.00	0.00	0.00	0.00	0.00	0.00	0.00	0.00
ZnO	0.18	ND	ND	ND	ND	5.04	ND	ND	ND	0.20
Li_2O	ND	ND	ND	ND	ND	ND	ND	ND	ND	ND
Total	100.67	100.54	99.96	100.24	100.04	99.90	99.68	100.06	100.70	99.11

	PYX 108	PYX 110	PYX 116	PYX 117	PYX 119	PYX 120	PYX 122	PYX 124	PYX 125	PYX 126
SiO_2	56.97	56.65	65.35	53.54	55.40	54.83	48.22	29.63	68.57	47.83
Al_2O_3	0.82	0.03	28.76	1.54	1.31	0.57	0.00	0.00	19.56	6.44
FeO	5.29	9.19	0.16	16.17	9.92	3.05	0.37	1.24	0.29	5.22
Fe_2O_3	1.13	0.44	ND	1.02	0.72	0.68	0.00	ND	ND	3.80
MgO	34.82	33.92	0.00	27.53	32.37	15.84	1.09	0.04	0.00	12.38
CaO	0.54	0.30	0.00	0.35	0.19	24.20	20.71	26.52	0.00	22.20
Na_2O	0.00	0.00	0.05	0.00	0.00	0.69	0.11	6.22	11.37	0.28
TiO_2	0.02	0.03	<0.01	0.03	0.04	0.04	0.00	1.01	0.01	1.32
Cr_2O_3	0.38	0.05	0.01	0.07	0.68	0.02	0.11	0.10	0.07	0.08
V_2O_5	0.00	0.01	0.00	0.00	0.00	0.00	0.01	0.00	0.00	0.03
CoO	0.02	0.01	0.00	0.01	0.03	0.04	0.08	0.15	0.04	0.05
NiO	0.05	0.02	0.00	0.05	0.05	0.04	0.09	0.14	0.01	0.04
MnO	0.18	0.04	0.03	0.44	0.26	0.35	27.27	0.62	0.01	0.16
ZrO_2	0.00	0.00	0.00	0.00	0.00	0.00	0.00	34.26	0.04	0.00
ZnO	ND	ND	ND	ND	ND	ND	1.68	ND	ND	ND
Li_2O	ND	ND	5.64[b]	ND	ND	ND	ND	ND	ND	ND
Total	100.22	100.69	100.00[a]	100.75	100.97	100.35	99.74	99.93	99.98	99.83

	PYX 128	PYX 130	PYX 132	PYX 134	PYX 150	PYX 152	PYX 153	PYX 170
SiO_2	51.25	53.42	53.61	55.59	55.75	47.00	56.30	52.49
Al_2O_3	0.90	0.23	0.27	1.08	0.24	0.00	9.03	4.48
FeO	3.59	0.04	0.37	0.22	2.56	7.54	3.31	2.62
Fe_2O_3	26.45	ND	8.19	0.00	0.00	0.00	ND	0.34
MgO	0.29	0.00	11.85	17.17	16.26	3.17	12.87	15.28
CaO	2.45	33.11	17.89	24.54	25.70	1.24	1.00	22.47
Na_2O	12.52	8.90	3.44	0.86	0.05	0.00	11.62	ND
TiO_2	0.43	0.00	0.01	0.02	0.00	0.06	0.18	0.04
Cr_2O_3	0.04	0.02	0.07	0.10	<0.01	0.02	3.41	0.99
V_2O_5	0.00	0.01	0.04	1.27	0.00	0.01	ND	0.16
CoO	0.04	0.01	0.03	0.03	0.05	0.09	0.07	0.00
NiO	0.00	0.04	0.02	0.03	<0.01	0.10	0.07	0.20
MnO	0.49	0.00	4.67	0.03	0.11	40.75	0.06	0.00
ZrO_2	1.86	0.00	0.00	0.00	<0.01	ND	ND	ND
ZnO	ND	ND	0.13	ND	0.03	0.15	ND	0.00
Li_2O	ND	ND	ND	ND	ND	0.00	0.04	ND
Total	100.31	95.78	100.59	100.94	100.75	100.13	97.96	99.07

[a] ND is not determined.
[b] Li_2O is assumed to be the difference between actual elemental abundances (as oxides) and 100%.

Ti^{3+}, Ti^{4+}, and Cr^{3+} [*Cameron and Papike*, 1980; *Rossman*, 1980; *Burns*, 1993]. Ti can also occupy the tetrahedral site [*Cameron and Papike*, 1980].

3.1. Cr-Bearing Pyroxenes

[13] *Hazen et al.* [1978] noted that a Cr-rich diopside from their study displayed its major absorption bands at longer than expected wavelengths on the basis of Fe and Ca content. *Cloutis and Gaffey* [1991] also suggested that the available Cr-rich samples used in their study displayed their major absorption band centers at longer than expected wavelengths relative to their Ca contents and shorter than expected wavelengths relative to their Fe contents. Existing data from *Adams* [1974], *Hazen et al.* [1978], *Cloutis and Gaffey* [1991], as well as new spectra acquired for this study have been examined to attempt to resolve this issue. The relationship between the actual and predicted band center positions for the major Fe^{2+} absorption bands near 1 and 2 μm are shown in Figures 2 and 3. The data suggest that there are no systematic offsets for the 1 μm band, while the

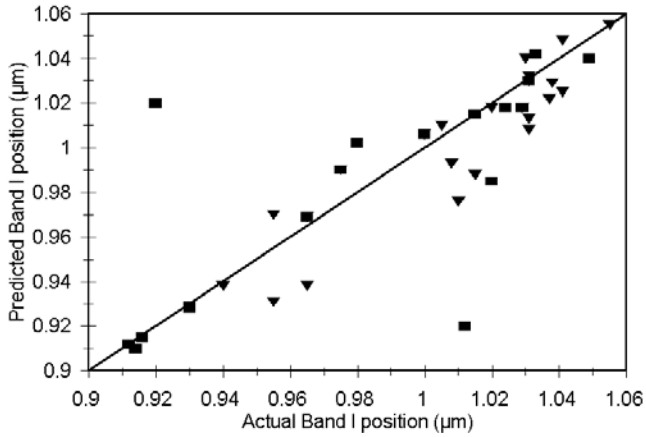

Figure 2. Predicted versus actual wavelength position of major Fe^{2+} absorption band centers in the 1 μm region for Cr-rich (squares) and Ti-rich (triangles) pyroxenes. The diagonal line represents the ideal case of a perfect match between predicted and observed band positions.

2 μm band center for the Cr-rich samples occur more frequently at longer than expected wavelengths versus shorter than expected wavelengths.

[14] Cr-rich pyroxenes also exhibit additional absorption bands at shorter wavelengths, associated with crystal field transitions in Cr^{3+} in the M1 site. Other oxidation states and site occupancies are also possible for chromium, including Cr^{2+} (in octahedral coordination), as well as Cr^{3+} and Cr^{4+} in tetrahedral coordination. These are rare in terrestrial pyroxenes but more common in lunar samples. These additional oxidation states and site occupancies can also give rise to crystal field transition bands [*Neuhaus*, 1960; *Mao et al.*, 1972; *Burns*, 1975; *Ikeda and Yagi*, 1977; *Schreiber*, 1977, 1978; *Ikeda and Yagi*, 1982; *Abs-Wurmbach et al.*, 1985; *Burns*, 1993].

[15] For Cr^{3+} in octahedral coordination in the M1 site, absorption bands in transmission spectra are seen in the

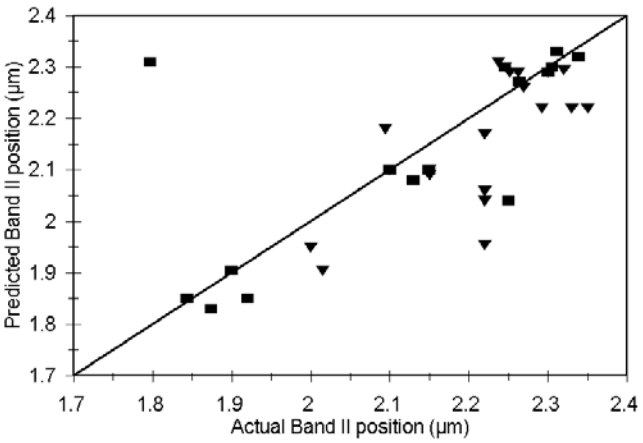

Figure 3. Predicted versus actual wavelength position of major Fe^{2+} absorption band centers in the 2 μm region for Cr-rich (squares) and Ti-rich (triangles) pyroxenes. The diagonal line represents the ideal case of a perfect match between predicted and observed band positions.

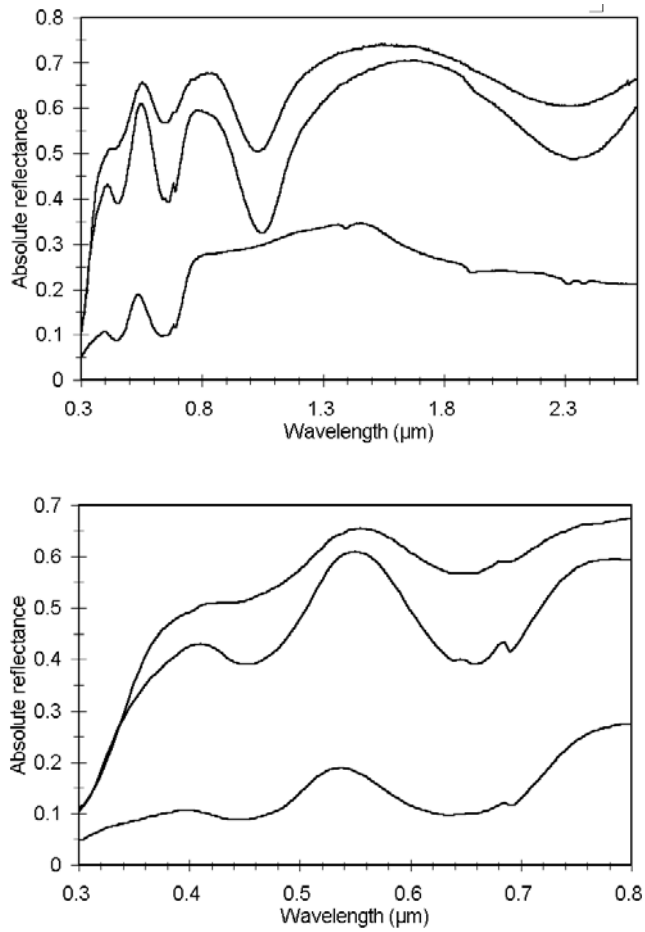

Figure 4. Reflectance spectra ((a) 0.3–2.6 μm; (b) 0.3–0.8 μm) of Cr-rich pyroxenes PYX 018 (middle spectrum), PYX 153 (bottom spectrum), and PYX 170 (top spectrum). Compositions are given in Table 1.

0.442–0.460 and 0.6–0.68 μm regions in both HCPs and LCPs [*Mao et al.*, 1972; *Rossman*, 1980; *Burns*, 1985; *Burns*, 1993]. In reflectance and transmission spectra, absorption bands have been noted near 0.45 and 0.65 μm, which increase in intensity with increasing Cr content [*Adams*, 1975; *Hazen et al.*, 1978].

[16] Figure 4 shows the reflectance spectra of three Cr-rich HCPs: two high-Ca samples (PYX 018: chrome diopside, PYX 170: diopside) and one Cr-Na LCP (PYX 153: ureyite) whose compositions are given in Table 1. Unlike Cr-poor pyroxenes, all three of these spectra exhibit an absorption band near 0.455 μm, as well as a more complex absorption feature in the 0.65 μm region, which consists of at least three absorption bands located at 0.64, 0.66, and 0.69 μm; these are most evident in the PYX 018 spectrum. This is consistent with previous results, and these bands are attributable to crystal field transitions in Cr^{3+} located in the M1 crystallographic site; the multiple bands arise from the splitting of the energy levels of the Cr^{3+} cation [e.g., *White et al.*, 1971; *Rossman*, 1980; *Burns*, 1985]. The reflectance spectra of *Adams* [1975] and *White et al.* [1971] do not show this level of complexity in the 0.65 μm region. However, high-resolution transmission spectra, as well as the current reflectance spectra,

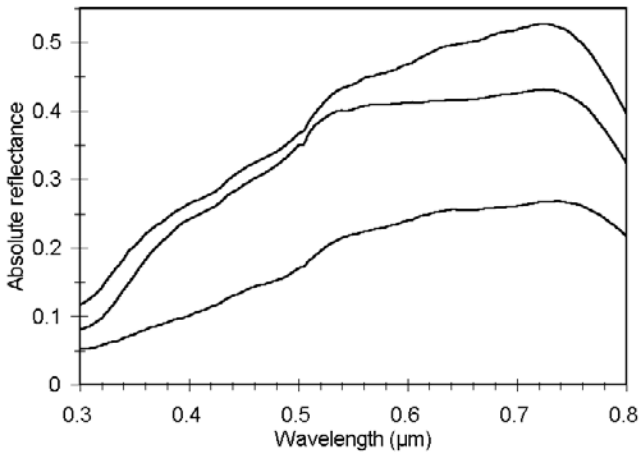

Figure 5. Reflectance spectra of three low-calcium pyroxenes containing 0.38 (PYX 108, top), 0.45 (PYX 023, middle), and 0.68 (PYX 119, bottom) wt % Cr_2O_3. Compositions are given in Table 1.

do show multiple bands in the 0.65 μm region [*Mao et al.*, 1972; *Rossman*, 1980; *Khomenko and Platonov*, 1985]. The 0.455 and 0.65 μm absorption features are only apparent in the HCP samples which contain >0.9 wt % Cr_2O_3. However, one terrestrial HCP sample was found which contains >1 wt % Cr_2O_3 and does not exhibit these Cr absorption features (not shown). This could be due to any number of factors such as a lower oxidation state (Cr^{2+}) or the Cr may be present in the tetrahaderal site or in some other phase (although there is no evidence of this from backscattered electron images). These results indicate that absorption features in the 0.455 and 0.65 μm regions (the latter being a complex absorption feature), when present, are indicative of octahedrally coordinated Cr^{3+} in the M1 site in abundances in excess of ~0.9 wt % Cr_2O_3. However, the absence of these bands may not necessarily be indicative of a Cr-poor pyroxene.

[17] Cr^{3+}-bearing LCP spectra exhibit similar behavior as the HCPs, with an absorption feature near 0.45 μm and a more complex absorption feature in the 0.6–0.68 μm region [*Rossman*, 1980]. These absorption features are also attributable to crystal field transitions in Cr^{3+} located in the M1 crystallographic site. Little chromium is needed to produce observable absorption bands in the 0.6–0.7 μm region of LCP spectra. LCPs with as little as 0.38 wt % Cr_2O_3 exhibit a broad absorption feature in the 0.6–0.7 μm region (Figure 5). This feature appears to be composed of at least two absorption bands, located near 0.60 and 0.67 μm, consistent with previous results [*Rossman*, 1980]. It should be noted that the Cr^{3+} absorptions in LCP spectra are much weaker than those seen in HCP spectra.

3.2. Ti-Bearing Pyroxenes

[18] Titanium generally occupies the M1 site in pyroxenes, and the Ti^{4+} oxidation state is much more common than the Ti^{3+} oxidation state in terrestrial pyroxenes [*Burns*, 1981]. Ti-rich samples were found by *Adams* [1974, 1975] to exhibit major absorption bands in the 1 and 2 μm regions at longer than expected wavelengths, as well as a suppression of a Fe^{2+} - Fe^{3+} charge transfer absorption near 0.77 μm. On the basis of a larger number of samples, *Cloutis and Gaffey* [1991] concluded that Ti-rich samples frequently plot off the trends relating band positions to Fe and Ca content, but that the offsets are neither systematic nor correlated with Ti content.

[19] Existing data from *Adams* [1974], *Hazen et al.* [1978], *Cloutis and Gaffey* [1991], as well as new spectra acquired for this study have been examined to attempt to resolve this issue. The relationship between the actual and predicted band center positions for the major Fe^{2+} absorption bands near 1 and 2 μm are shown in Figures 2 and 3. The data suggest that both the major absorption bands are generally shifted to longer than expected wavelengths, and the magnitude of this offset is greater for the 2 μm band.

[20] In terms of minor absorption bands, Ti^{3+}-bearing minerals exhibit absorption features in the 0.455–0.475 and 0.605–0.640 μm regions due to crystal field transitions in Ti^{3+} located in the M1 crystallographic site [*Burns*, 1993]. Note that these regions are similar to those assigned to Cr^{3+} crystal field transitions as described in section 3.1. For Ti^{4+}-bearing minerals, absorption features due to Ti^{3+}-Ti^{4+} and Fe^{2+}-Ti^{4+} intervalence charge transfers are possible [*Burns*, 1981; *Sherman*, 1987; *Mattson and Rossman*, 1988]. Such transitions have been found in pyroxenes from the Allende carbonaceous chondrite meteorite (Ti^{3+}-Ti^{4+}) and in titanaugites (Fe^{2+}-Ti^{4+}) [*Burns*, 1981]. Ti^{3+}-Ti^{4+} charge transfers give rise to absorption bands near 0.50 and 0.65 μm, while Fe^{2+}-Ti^{4+} charge transfers give rise to a broad absorption band in the 0.43–0.485 μm region [*Burns et al.*, 1976; *Burns*, 1981, 1993].

[21] The reflectance spectra of available Ti-rich samples (>1 wt% TiO_2), all of which are HCPs, exhibit an absorption band near 0.46 μm (Figure 6). The position of this band is outside of the ranges associated with various Fe^{2+} and Fe^{3+} charge transfer, crystal field, and intervalence charge transfer bands [*Bell and Mao*, 1972a, 1972b; *Abu-Eid*, 1976; *Abu-Eid and Burns*, 1976; *Amthauer and Rossman*, 1984] and is only present at this position in the Ti-rich samples. This strongly suggests that this band is attributable to a Fe^{2+}-Ti^{4+} charge transfer and can be detected in the reflectance spectra of Ti^{4+}-bearing HCPs. The absorption feature present near 0.75 μm is probably attributable to Fe^{2+}-Fe^{3+} charge transfers (see section 3.10).

3.3. V-Bearing Pyroxenes

[22] Vanadium can be present in a number of oxidation states, with the V^{2+}, V^{3+}, and V^{4+} ions possessing unpaired electrons which can give rise to crystal field transition absorption bands [*Burns*, 1993]. The spectrum of lavrovite, a V-rich diopside (1.27 wt % V_2O_5) is shown in Figure 7. It exhibits a weak absorption band in the 1 μm region and a largely indistinguishable band in the 2 μm region (also partially obscured by the sharp absorption bands because of incipient alteration), consistent with its low iron content (Table 1). It also exhibits two stronger absorption bands near 0.445 and 0.680 μm, which are probably attributable to crystal field transitions in V^{3+} located in the M1 site [*Schmetzer*, 1982; *Carlson and Rossman*, 1988; *Burns*, 1993]. This is in contrast to Ti^{4+} which exhibits only one band, and Cr^{3+} which exhibits more than two bands (Table 2). These bands can be used to identify the presence of V-bearing pyroxenes. The minor absorption bands in the

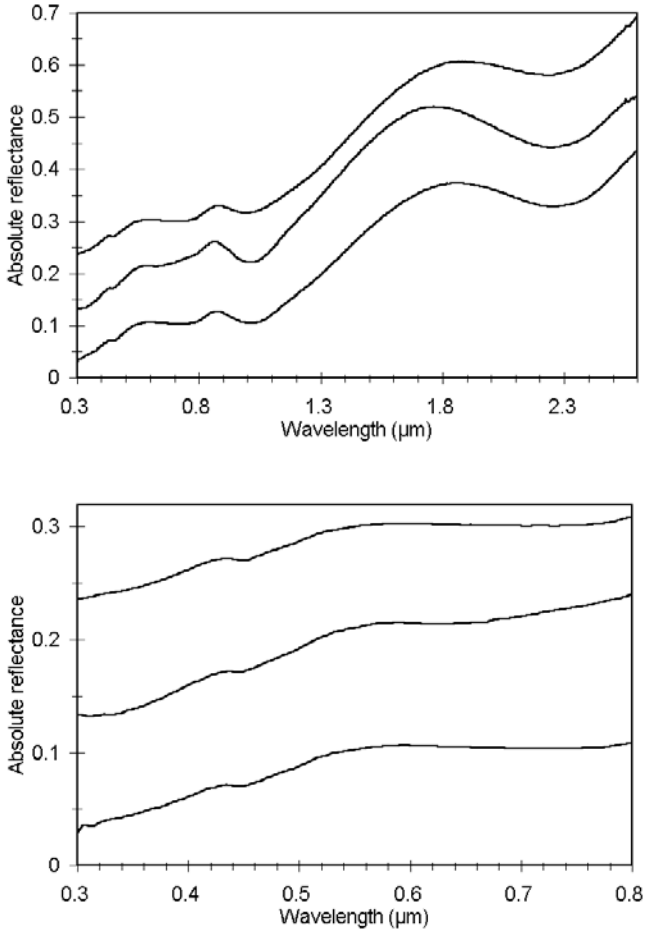

Figure 6. Reflectance spectra ((a) 0.3–2.6 μm; (b) 0.3–0.8 μm) of Ti-rich pyroxenes PYX 035 (bottom curve), PYX 040 (middle curve), and PYX 126 (top curve). The PYX 040 and PYX 126 have been offset vertically by +0.1 and +0.2, respectively, for clarity. Compositions are given in Table 1.

1.4 and 2.3 μm regions are due to a small amount of alteration in the sample.

3.4. Mn- and Zn-Bearing Pyroxenes

[23] Manganese can occur in pyroxenes in a variety of oxidation states [*Burns*, 1993]. Mn^{3+} is expected to exhibit a series of absorption bands roughly comparable to Fe^{2+}, as their electronic configurations are similar, with the Mn strongly partitioned into the M1 site [*Abu-Eid*, 1976; *Langer and Abu-Eid*, 1977]. Mn^{2+} should not give rise to crystal field transition bands as it does not possess unpaired electrons. Reflectance spectra of three presumed Mn^{3+}-bearing pyroxenes (on the basis of their ideal formulas) are shown in Figure 8 (PYX 013: urbanite; PYX 033: Mn-augite; PYX 132: schefferite). With the exception of some absorption bands in the 1.4 and 2.3 μm regions due to incipient alteration, the reflectance spectra are relatively featureless; only the PYX 033 spectrum, the most Fe^{2+}-rich of the three samples (Table 1), exhibits Fe^{2+} absorption bands in the 1 μm region. All three spectra exhibit an absorption feature near 0.77 μm, which is probably attributable to Fe^{2+}-Fe^{3+} intervalence charge transfers. Expected absorption bands for Mn^{3+} near 0.6 μm are not evident. This may be due to the relatively low abundances of Mn in the samples (Table 1), the presence of Mn in the M2 site, or the Mn may be present in the Mn^{2+} or Mn^{4+} oxidation states, which would not give rise to crystal field transition absorption bands. In addition, the presence of appreciable Zn in sample PYX 033 (5.04 wt % ZnO) does not result in any identifiable absorption features.

[24] Reflectance spectra of three other Mn-rich pyroxenes (PYX 044: rhodonite, PYX 122: bustamite; PYX 152: pyroxmangite/rhodonite) are shown in Figure 9. The Mn in these samples is presumed to be in the Mn^{2+} oxidation state on the basis of their ideal formulas. However, all three samples exhibit absorption features characteristic of Mn^{3+}. In particular, the PYX 122 spectrum exhibits a broad absorption band near 1.5 μm, attributable to crystal field transitions in Mn^{3+} present in the M1 site [*Ghose et al.*, 1986]. Absorption bands attributable to Fe^{2+} crystal field transitions are only apparent in the PYX 152 sample, the most iron-rich of the three.

[25] All three spectra exhibit a number of absorption features below 0.6 μm. Resolvable bands are present at 0.345, 0.360, 0.410–0.420, 0.440, 0.505, and 0.540 μm in at least one of the three spectra. The bands at 0.360, 0.410, 0.440, and 0.505 μm are assigned to spin-forbidden bands in Mn^{2+} and Fe^{3+} by *Ghose et al.* [1986]. The identity of the band at 0.345 μm is unknown.

[26] These three samples span a range of compositions. PYX 044 is essentially iron- and calcium-free, PYX 122 is an HCP and nearly iron-free, and PYX 152 is essentially calcium-free but contains ferrous iron and no ferric iron. On the basis of the appearance of the various absorption bands, the compositions of the samples and the preference of Mn^{3+} for the M1 site in LCPs, it seems reasonable to assign the bands at 0.345, 0.360, 0.410, and 0.540 μm (which appear in the LCP samples PYX 044 and PYX 152) to crystal field transitions in Mn^{3+} located in the M1 crystallographic site; the band at 0.505 μm to a ferrous iron spin-forbidden crystal field transition (see section 3.9), as it only appears in the ferrous iron-bearing sample spectrum (PYX 122); and the bands at 0.420 and 0.440 to crystal field transitions in Mn^{3+}

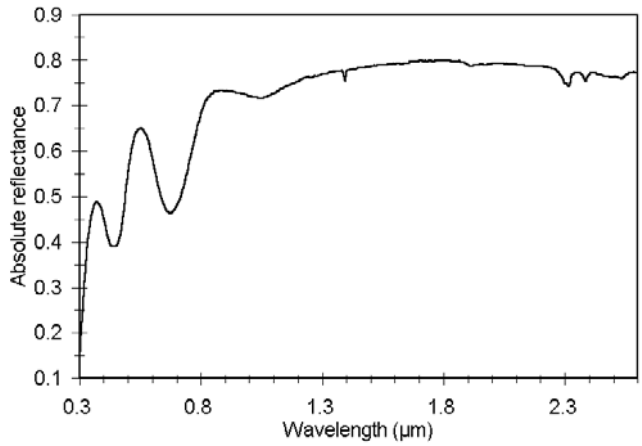

Figure 7. Reflectance spectrum of a V-rich high-calcium pyroxene (PYX 134). Composition is given in Table 1.

Table 2. Absorption Bands Associated With Various Cations in Pyroxenes

Cation and Site Occupancy	Mechanism	Location of Associated Absorption Bands, μm
Cr^{3+} in M1 octahedral site in HCP	Crystal field transitions	0.455, 0.64, 0.66, 0.69[a]
Cr^{3+} in M1 octahedral site in LCP	Crystal field transitions	0.45, 0.60, 0.67
Ti^{4+} in M1 octahedral site in HCP	Fe^{2+}-Ti^{4+} charge transfer	0.46
V^{3+} in M1 octahedral site in HCP	Crystal field transitions	0.445, 0.680
Mn^{3+} in M1 octahedral site in LCP	Crystal field transitions	0.345, 0.360, 0.410, 0.540, 1.5
Mn^{3+} in M1 octahedral site in HCP	Crystal field transitions	0.420, 0.440
Zr		No diagnostic absorption bands
Li		No diagnostic absorption bands
Na		No diagnostic absorption bands
Ca		No diagnostic absorption bands
Fe^{2+} in M2 octahedral site in LCP	Spin-forbidden crystal field transitions	0.425, 0.445, 0.480, 0.505, 0.545
Fe^{3+} in octahedral sites in LCP	Fe^{2+} - Fe^{3+} charge transfer	0.69
Fe^{3+} in octahedral sites in HCP	Fe^{2+} - Fe^{3+} charge transfer	0.73

[a] The latter three bands may only appear as an unresolved broad absorption feature.

located in the M1 crystallographic site in the clinopyroxene structure, as these bands only appear in the PYX 122 spectrum, and this is the preferred site for Mn^{3+} [*Burns*, 1993]. Regardless of the precise site assignments for Mn^{3+}, it appears that the multiplicity of bands in the Mn-bearing pyroxenes is unique to these minerals and allows for their identification.

3.5. Zr-Bearing Pyroxenes

[27] Wöhlerite is a Zr-rich pyroxene group mineral (PYX 124), and its reflectance spectrum is shown in Figure 10. It exhibits a typical type A HCP reflectance spectrum, i.e., an absorption feature in the 1 μm region, as expected for a Ca-rich pyroxene. The presence of appreciable Zr in this sample (Table 1) does not appear to affect the reflectance spectrum. The wavelength position of the 1 μm band is consistent with that of diopsides of similar Fe^{2+} content.

3.6. Li-Bearing Pyroxenes

[28] Li-rich pyroxene (spodumene) contains Li and Al in place of Fe, Mg, and Ca. The reflectance spectrum of spodumene is shown in Figure 11. As expected, its reflectance spectrum is nearly featureless, as there are no mechanisms for the Li and Al to contribute absorption bands in the 0.3–2.6 μm region.

3.7. Na-Bearing Pyroxenes

[29] There are a number of Na-bearing pyroxene group minerals. The reflectance spectra of three members, jadeite

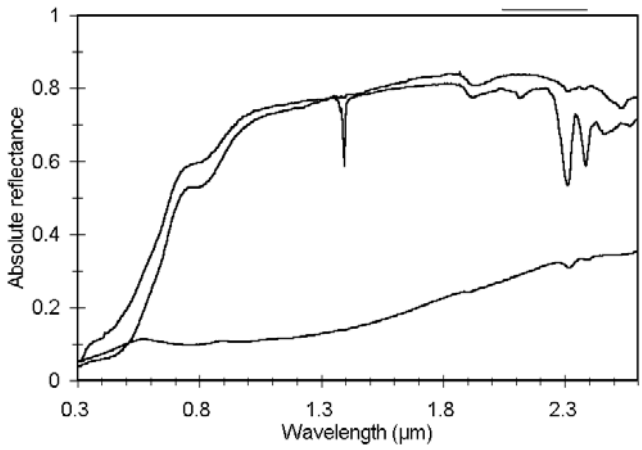

Figure 8. Reflectance spectra of Mn-rich pyroxenes PYX 013 (top spectrum at 0.8 μm), PYX 033 (bottom spectrum at 0.8 μm), and PYX 132 (middle spectrum at 0.8 μm). Compositions are given in Table 1.

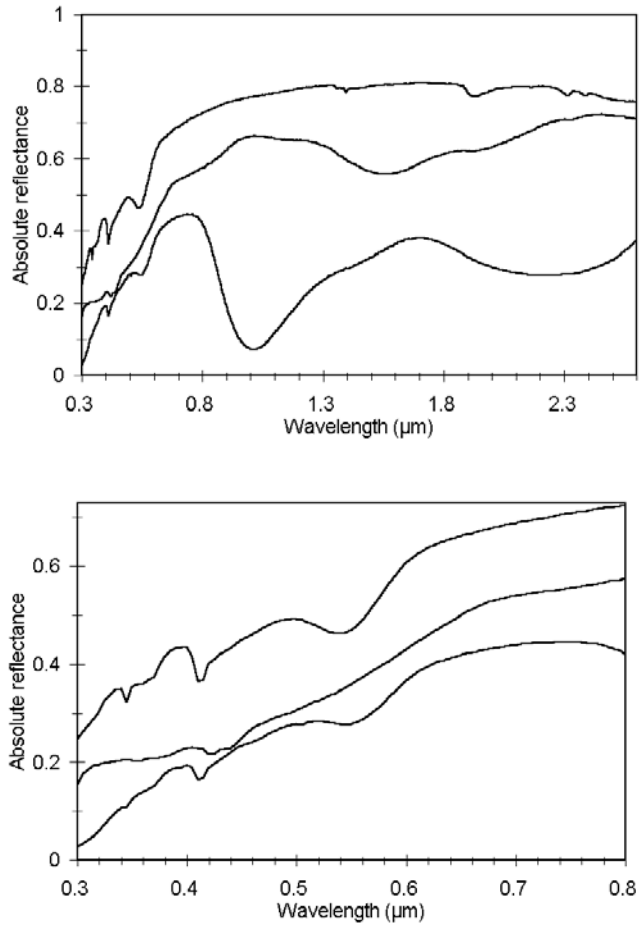

Figure 9. Reflectance spectra ((a) 0.3–2.6 μm; (b) 0.3–0.8 μm) of Mn-rich pyroxenes PYX 044 (top spectrum), PYX 122 (middle spectrum), and PYX 152 (bottom spectrum). The PYX 152 spectrum has been offset by −0.05 for clarity. Compositions are given in Table 1.

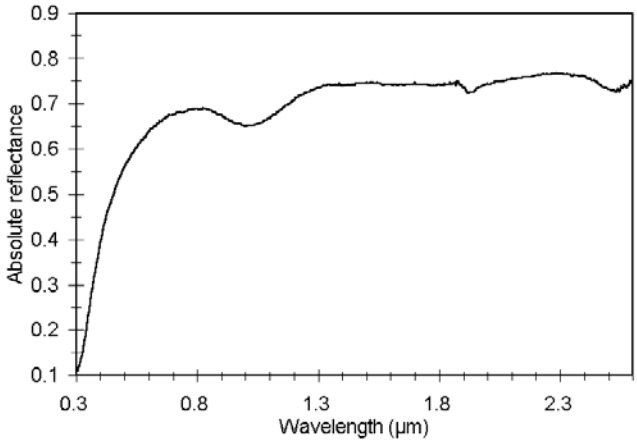

Figure 10. Reflectance spectrum of Zr-rich pyroxene PYX 124. Composition is given in Table 1.

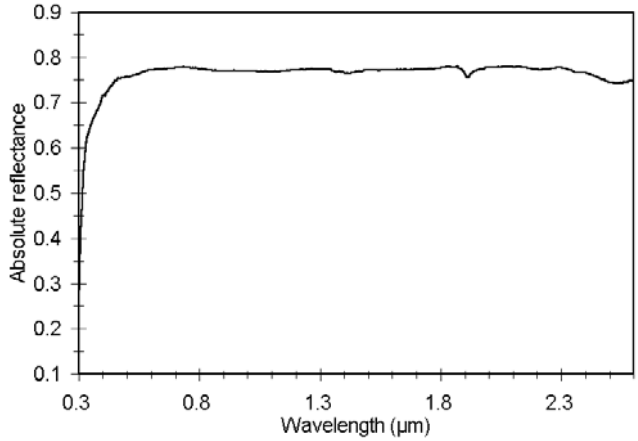

Figure 11. Reflectance spectrum of Li-rich pyroxene PYX 116 (spodumene). Composition is given in Table 1.

(PYX 125; ideal formula $NaAlSi_2O_6$), aegerine (PYX 128; ideal formula $NaFe^{3+}Si_2O_6$), and pectolite (PYX 130; ideal formula $Ca_2NaH(SiO_3)_3$) are shown in Figure 12, and their compositions are provided in Table 1. The jadeite spectrum is relatively flat and featureless, consistent with the lack of transition series elements. The aegerine spectrum is similar to hedenbergite spectra, with low overall reflectance in the visible region and reflectance gradually rising toward longer wavelengths. It exhibits a broad absorption band in the 0.75 μm region, consistent with Fe^{2+}-Fe^{3+} intervalence charge transfers (the sample contains both ferrous and ferric iron; see Table 1) [*Amthauer and Rossman*, 1984]. It also exhibits a broad absorption feature in the 1.1 μm region, consistent with Fe^{2+} crystal field transitions. The overall spectral shape and lack of an absorption band in the 2 μm region are consistent with type A HCPs [*Adams*, 1975]. The reflectance spectrum of pectolite is very distinctive. It is characterized by high overall reflectance below ~1.4 μm, and progressively decreasing reflectance toward longer wavelengths. This reflectance decline probably represents the short-wavelength wing of an intense O-H stretching fundamental band near 2.8 μm [*Hunt and Salisbury*, 1970].

3.8. Ca-Dominated Pyroxenes

[30] Wollastonite is the Ca end-member of the pyroxene compositional tetralateral. Reflectance spectra of two wollastonite samples are shown in Figure 13. As expected, the reflectance spectra are characterized by high overall reflectance and no appreciable absorption bands, since elemental substitutions are usually minor in this mineral. The broad, weak absorption features in the 1 and 2 μm regions are probably due to the minor amounts of Fe^{2+} that may be present in the samples.

3.9. Fe^{2+} Minor Absorption Bands

[31] Most LCPs and some HCPs exhibit a number of minor absorption bands in the 0.4–0.6 μm wavelength region. These bands are invariably located near 0.425, 0.445, 0.480, 0.505, and 0.545 μm (Figure 14). They have been studied by a number of investigators, and there is broad agreement that most or all of these bands are attributable to spin-forbidden crystal field transitions in Fe^{2+} located in the M2 crystallographic site [*Runciman et al.*, 1973; *Abu-Eid*, 1976; *Langer and Abu-Eid*, 1977; *Goldman and Rossman*, 1979; *Hazen et al.*, 1978; *Zhao et al.*, 1986; *Burns*, 1993]. The present work demonstrates that these minor absorption bands are readily resolvable in reflectance spectra of powdered LCPs. Other minor absorption bands in the visible region spectra of LCPs, attributable to other mechanisms such as Fe^{3+} crystal field transitions, or other cations, are not apparent, probably because of the low abundances of Fe^{3+} and other cations in these samples (Table 1).

[32] By contrast, few HCP reflectance spectra exhibit comparable absorption bands in this wavelength region. This is attributable to the fact that Fe^{2+} preferentially occupies the M2 site in LCPs, while the M2 site in HCPs is preferentially occupied by Ca. Thus Fe^{2+} occupancy of the M2 site is normally much lower in HCPs than in LCPs.

3.10. Fe^{2+}-Fe^{3+} Intervalence Charge Transfer Absorption Bands

[33] The presence of both ferrous and ferric iron in pyroxenes can give rise to Fe^{2+}-Fe^{3+} intervalence charge

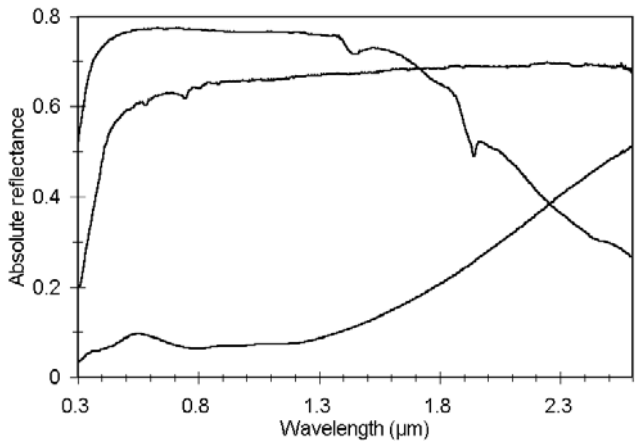

Figure 12. Reflectance spectra of Na-rich pyroxenes jadeite (PYX 125, middle spectrum at 0.5 μm), aegerine (PYX 128, bottom spectrum at 0.5 μm), and pectolite (PYX 130; top spectrum at 0.5 μm). Compositions are given in Table 1.

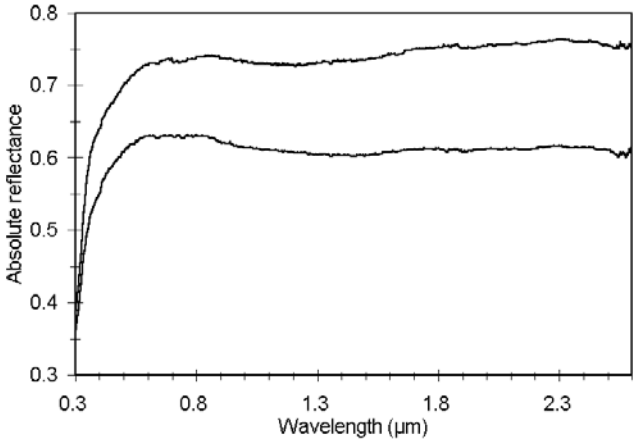

Figure 13. Reflectance spectra of two Ca-rich pyroxenes (wollastonites), PYX 180 (top spectrum) and PYX 182 (bottom spectrum). The PYX 182 spectrum has been vertically offset by −0.1 for clarity.

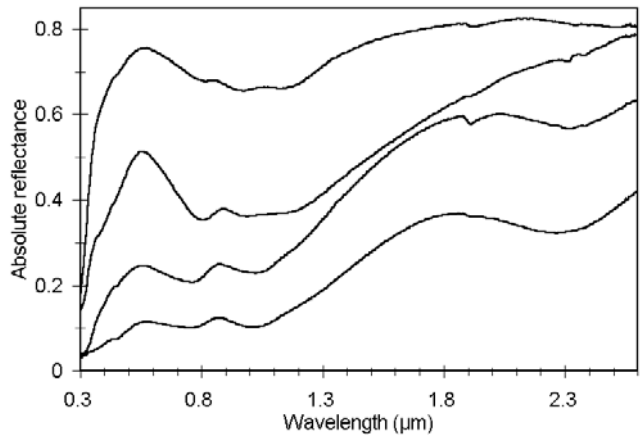

Figure 15. Reflectance spectra of high-calcium pyroxenes exhibiting ferrous-ferric intervalence charge transfer bands in the 0.75–0.80 μm region. Sample spectra in order from bottom to top at 0.5 μm: PYX 019, PYX 029, PYX 120, PYX 150. The PYX 120 spectrum has been vertically offset by +0.1 for clarity. Compositions are given in Table 1.

transfer absorption bands. In LCP transmission spectra this feature is present near 0.69 μm, while in HCP transmission spectra it is present near 0.73 μm [*White and Keester*, 1966; *Burns and Huggins*, 1973; *Amthauer and Rossman*, 1984; *Burns*, 1981; *Steffen et al.*, 1988; *Burns*, 1993]. The reflectance spectra of the LCPs included in this study do not exhibit a resolvable absorption feature in this region probably because of the low Fe^{3+} content of the samples.

[34] Most HCP reflectance spectra exhibit an Fe^{2+}-Fe^{3+} intervalence charge transfer absorption band in the 0.75–0.8 μm region (Figure 15). This feature is most evident in those samples that contain at least a few weight percent of both ferrous and ferric iron. In more iron-rich samples, this feature is usually less evident, probably because of lower overall reflectance in this wavelength region. Because of this effect, there is no apparent relationship between the depth of this band and ferrous, ferric, or total iron content. This band appears in both type A and type B HCP spectra, and there is no systematic difference in the wavelength position of this band between the two spectral types.

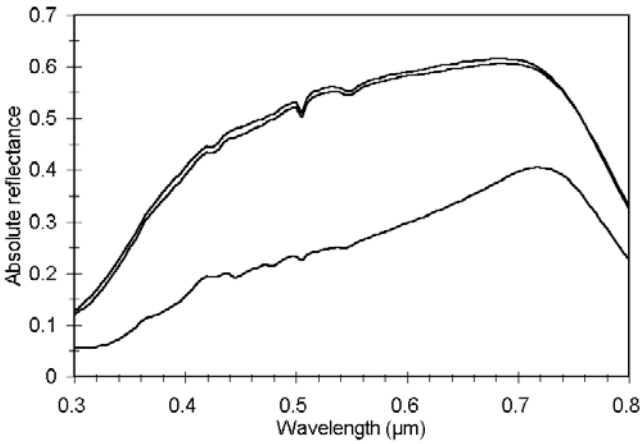

Figure 14. Reflectance spectra of three low-calcium pyroxenes showing a series of Fe^{2+} spin-forbidden crystal field transition bands: PYX 110 (top spectrum), PYX 042 (middle spectrum), PYX 117 (bottom spectrum). Compositions are given in Table 1.

4. Discussion

[35] The presence of transition series elements, such as Cr, Ti, V, and Mn, with valences which result in unfilled orbitals, and in abundances on the order of >∼1% of the equivalent oxide, give rise to absorption features which are unique to a particular cation. Cr^{3+}, which is normally present in the M1 site, gives rise to an absorption band near 0.455 μm and a more complex absorption feature in the 0.65 μm region. The presence of Ti^{4+} in pyroxenes gives rise to an absorption band near 0.46 μm, attributable to Fe^{2+}-Ti^{4+} charge transfers. V^{3+}, which preferentially occupies the M1 crystallographic site, results in absorption bands near 0.445 and 0.680 μm, attributable to crystal field transitions. Manganese-rich samples are characterized by a number of absorption bands in the 0.3–0.6 μm region, as well as an absorption band near 1.5 μm in some cases. The bands at 0.54 and 1.5 μm are attributed to crystal field transitions in Mn^{3+}.

[36] The presence of other cations, which are not transition series elements, such as Zn, Zr, Li, Na, and Ca, do not give rise to absorption bands in the 0.3–2.6 μm region. Pyroxene-group minerals such as wollastonite (the Ca-rich end-member), spodumene, and jadeite are spectrally quite featureless, because of their lack or low abundance of transition series elements. Pectolite spectra are dominated by the presence of H in their structure, while other sample spectra, such as wöhlerite and aegerine, only exhibit features associated with the transition series elements that are present. The various unique spectral features associated with the various minor elements and cations examined in this study are summarized in Table 2.

[37] Ideally, we would like to be able to use various properties of these absorption bands, such as depths and widths, to constrain the abundances of the various cations. However, in most cases, either insufficient samples were

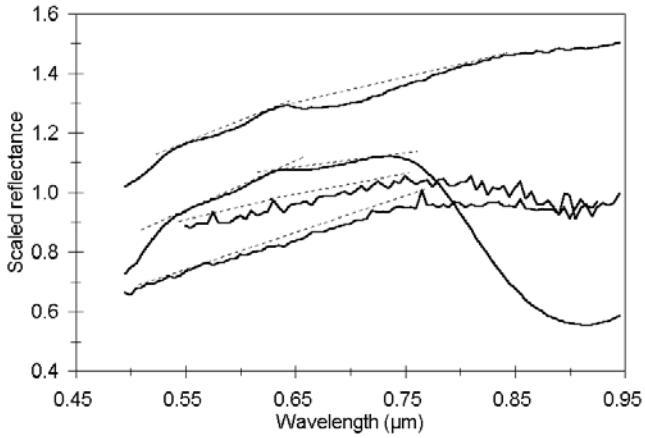

Figure 16. Reflectance spectra of two S-class asteroids which show evidence for absorption features in the 0.6–0.7 μm region (292 Ludovica and 692 Hippodamia), the Cr-bearing pyroxene PYX 119, and a chromite. All spectra have been normalized at 0.7 μm. Some of the spectra have also been linearly vertically offset for clarity. The spectra from bottom to top at 0.7 μm and the vertical offsets are as follows: 292 Ludovica (−0.1 vertical offset), 692 Hippodamia (no vertical offset), PYX 119 (+0.1 vertical offset), and chromite (+0.3 vertical offset). Straight-line continua (dashed lines) are also shown in order to highlight some of the minor absorption bands.

available, or were not compositionally diverse enough, to permit the derivation of quantitative spectral-compositional relationships. In addition, in practical remote-sensing situations, we would not normally expect monomineralic pyroxene occurrences to be widely present. The presence of accessory phases would complicate the derivation of minor cation abundances through processes such as a reduction in absorption band depths and widths due to accessory opaque phases [e.g., *Cloutis et al.*, 1990; *Cloutis and Bell*, 2000]. In addition, changes in the grain size of the pyroxenes will also have an effect on the depth of these absorption bands [*Cloutis and Gaffey*, 1991; *Sunshine and Pieters*, 1993]. Consequently, the presence of specific absorption bands can be taken as evidence for the presence of a particular cation, but the characteristics of these bands are probably not reliable for constraining cation abundance.

[38] LCP spectra commonly exhibit a series of absorption bands in the visible wavelength region which are mostly attributable to spin-forbidden crystal field transitions in Fe^{2+} located in the M2 crystallographic site. These bands are evident in LCP reflectance spectra, but less so in HCP spectra, probably because of their lower Fe^{2+} M2 site occupancy. The number and wavelength positions of this suite of bands is unique to spin-forbidden crystal field transitions in Fe^{2+} located in the M2 crystallographic site. Fe^{2+}-Fe^{3+} intervalence charge transfer transition absorption features can also appear in both LCP and HCP reflectance spectra when both ferrous and ferric iron are present at abundances $>\sim$1 wt %. The wavelength position of this band is different in LCPs ($\sim$0.65 μm) versus HCPs ($\sim$0.75–0.80 μm) and can be used to detect the presence of spectrally significant amounts of ferric iron. This feature is present in both type A and type B HCP spectra.

5. Remote-Sensing Applications

[39] Minor absorption bands in pyroxene reflectance spectra have been, and can be, used for compositional studies. *Cochran and Vilas* [1998] have measured changes in the appearance of the spin-forbidden crystal field transition band of Fe^{2+} located near 0.506 μm to map surficial variations in pyroxene mineralogy of asteroid 4 Vesta. The wavelength position and shape of this band (singlet or doublet) is diagnostic of pyroxene Ca content [*Hazen et al.*, 1978]. This absorption band, while well resolved in the LCP reflectance spectra (Figure 14), is only poorly resolved in some HCP spectra. This is probably attributable to the lower abundance of Fe^{2+} in the M2 site of HCPs, as well as the fact that the spectral resolution of the current laboratory spectra (5 nm) hampers detailed analysis of such narrow absorption features.

[40] *Hiroi et al.* [1996] detected minor absorption bands, centered near 0.6 and 0.67 μm, in the reflectance spectra of a number of S-asteroids. They interpreted these bands as being most consistent with oxidized Fe-Ni metal and spinel-group minerals, respectively. Similar bands are seen in the reflectance spectra of pyroxene-rich meteorites such as diogenites [*Gaffey*, 1976; *McFadden et al.*, 1982]. *McFadden et al.* [1982] assigned the absorption band at 0.60 μm to Cr^{3+} in pyroxene, and the 0.65–0.67 μm band to chromite, which was present in the diogenite samples.

[41] As discussed in section 3.1, little chromium is needed to produce observable absorption bands in the 0.6–0.7 μm region of LCP spectra (Figure 5). This wavelength region appears to contain at least two absorption bands, located near 0.60 and 0.67 μm, similar to the bands seen in the S-asteroid and diogenite spectra. By contrast, chromite spectra exhibit more complex absorption features, with absorption bands located near 0.495, 0.595, and a double band at 0.67 and 0.695 μm (Figure 16). A double-band structure is not apparent in the 0.67–0.695 μm region of the S-asteroid spectra but could be present. Band depths in the LCP spectra are comparable to those seen in the S-asteroid spectra (a few percent). Thus the two bands seen in the S-asteroid spectra are consistent with Cr^{3+}-bearing LCP and/or chromite. Given that LCP is a major component of most S-asteroids [*Gaffey et al.*, 1993], the presence of Cr-bearing LCP on the surfaces of these asteroids is reasonable.

6. Conclusions

[42] Absorption features present below 0.8 μm in LCP and HCP reflectance spectra can be used to determine the presence of various transition series cations such as Fe^{2+}, Fe^{3+}, Cr^{3+}, Ti^{4+}, and V^{3+}. Absorption bands attributable to these cations generally become evident when the abundances of these cations exceed $\sim$1 wt % as their equivalent oxide. The range of cation-associated features seen in the reflectance spectra of the current samples, as well as the results of spectroscopic studies of asteroid 4 Vesta and some S-asteroids, indicate that reflectance spectroscopy can be successfully applied to detailed compositional studies of pyroxene-bearing remote surfaces.

[43] **Acknowledgments.** This study was supported by grants-in-aid of research from the Natural Sciences and Engineering Research Council of

Canada (NSERC), Sigma Xi, The Scientific Research Society, the Geological Society of America, a research contract from the Canadian Space Agency, and a start-up grant from the University of Winnipeg. Thanks to E. D. Ghent and John Machacek of the University of Calgary electron microprobe facility, Alex Stelmach and Diane Caird of the University of Alberta for their kind assistance in characterizing the samples, and Carlé Pieters, Stephen Pratt, and Takahiro Hiroi for generously providing access to the NASA-supported multiuser RELAB spectrometer facility at Brown University. Thanks to Jessica Sunshine and Kevin Reed for their many helpful suggestions for improving this manuscript.

References

Abs-Wurmbach, I., K. Langer, and R. Oberhänsli, Polarized absorption spectra of single crystals of the chromium-bearing clinopyroxenes kosmochlor and Cr-aegerine-augite, *Neues Jahrb. Mineral. Abh.*, *152*, 293–319, 1985.

Abu-Eid, R. M., Absorption spectra of transition metal-bearing minerals at high pressures, in *The Physics and Chemistry of Minerals and Rocks*, edited by R. G. J. Strens, pp. 641–675, John Wiley, New York, 1976.

Abu-Eid, R. M., and R. G. Burns, The effect of pressure on the degree of covalency of the cation-oxygen bond in minerals, *Am. Mineral.*, *61*, 391–397, 1976.

Adams, J. B., Visible and near-infrared diffuse reflectance spectra of pyroxenes as applied to remote sensing of solid objects in the solar system, *J. Geophys. Res.*, *79*, 4829–4836, 1974.

Adams, J. B., Interpretation of visible and near-infrared diffuse reflectance spectra of pyroxenes and other rock-forming minerals, in *Infrared and Raman Spectroscopy of Lunar and Terrestrial Minerals*, edited by C. Karr Jr., pp. 91–116, Academic, San Diego, Calif., 1975.

Amthauer, G., and G. R. Rossman, Mixed valence of iron in minerals with cation clusters, *Phys. Chem. Miner.*, *11*, 37–51, 1984.

Angel, R. J., T. Gasparik, and L. W. Finger, Crystal structure of a Cr^{2+}-bearing pyroxene, *Am. Mineral.*, *74*, 599–603, 1989.

Bancroft, G. M., and R. G. Burns, Interpretation of the electronic spectra of iron in pyroxenes, *Am. Mineral.*, *52*, 1278–1287, 1967.

Bancroft, G. M., R. G. Burns, and R. A. Howie, Determination of the cation distribution in the orthopyroxene series by the Mossbauer effect, *Nature*, *213*, 1221–1223, 1967a.

Bancroft, G. M., A. G. Maddock, and R. G. Burns, Applications of the Mössbauer effect to silicate mineralogy, I, Iron silicates of known crystal structure, *Geochim. Cosmochim. Acta*, *31*, 2219–2246, 1967b.

Basaltic Volcanism Study Project, *Basaltic Volcanism on the Terrestrial Planets*, Pergamon, New York, 1981.

Bell, P. M., and H. K. Mao, Crystal-field effects of iron and titanium in selected grains of Apollo 12, 14, and 15 rocks, glasses and fine fractions, *Proc. Lunar Sci. Conf.*, *3rd*, 545–553, 1972a.

Bell, P. M., and H. K. Mao, Crystal-field determination of Fe^{3+}, *Year Book Carnegie Inst. Washington*, *71*, 531–534, 1972b.

Burns, R. G., *Mineralogical Applications of Crystal Field Theory*, Cambridge Univ. Press, New York, 1970.

Burns, R. G., On the occurrence and stability of divalent chromium in olivines included in diamonds, *Contrib. Mineral. Petrol.*, *51*, 213–221, 1975.

Burns, R. G., Intervalence transitions in mixed-valence minerals of iron and titanium, *Ann. Rev. Earth Planet. Sci.*, *9*, 345–383, 1981.

Burns, R. G., Thermodynamic data from crystal field spectra, in *Reviews in Mineralogy*, vol. 14, *Microscopic to Macroscopic: Atomic Environments to Mineral Thermodynamics*, edited by S. W. Kieffer and A. Navrotsky, pp. 277–316, Mineral. Soc. of Am., Washington, D. C., 1985.

Burns, R. G., *Mineralogical Applications of Crystal Field Theory*, 2nd ed., Cambridge Univ. Press, New York, 1993.

Burns, R. G., and F. E. Huggins, Visible-region absorption spectra of a Ti^{3+} fassaite from the Allende meteorite: A discussion, *Am. Mineral.*, *58*, 955–961, 1973.

Burns, R. G., F. E. Huggins, and R. M. Abu-Eid, Polarized absorption spectra of single crystals of lunar pyroxenes and olivines, *Moon*, *4*, 93–102, 1972a.

Burns, R. G., R. Abu-Eid, and F. E. Huggins, Crystal field spectra of lunar pyroxenes, *Proc. Lunar Sci. Conf.*, *3rd*, 533–543, 1972b.

Burns, R. G., K. M. Parkin, B. M. Loeffler, I. S. Leung, and R. M. Abu-Eid, Further characterization of spectral features attributable to titanium on the moon, *Proc. Lunar Sci. Conf.*, *7th*, 2561–2578, 1976.

Cameron, M., and J. J. Papike, Crystal chemistry of silicate pyroxenes, in *Reviews in Mineralogy*, vol. 7, *Pyroxenes*, edited by C. T. Prewitt, pp. 5–92, Mineral. Soc. of Am., Washington, D. C., 1980.

Carlson, W. D., and G. R. Rossman, Vanadium- and chromium-bearing andalusite: Occurrence and optical-absorption spectroscopy, *Am. Mineral.*, *73*, 1366–1369, 1988.

Clark, S. P., Jr., Absorption spectra of some silicates in the visible and near-infrared, *Am. Mineral.*, *42*, 732–742, 1957.

Cloutis, E. A., and J. F. Bell III, Diaspores and related hydroxides: Spectral-compositional properties and implications for Mars, *J. Geophys. Res.*, *105*, 7053–7070, 2000.

Cloutis, E. A., and M. J. Gaffey, Pyroxene spectroscopy revisited: Spectral-compositional correlations and relationship to geothermometry, *J. Geophys. Res.*, *96*, 22,809–22,826, 1991.

Cloutis, E. A., M. J. Gaffey, D. G. W. Smith, and R. S. J. Lambert, Reflectance spectra of mafic silicate-opaque assemblages with applications to meteorite spectra, *Icarus*, *84*, 315–333, 1990.

Cochran, A. L., and F. Vilas, The changing spectrum of Vesta: Rotationally resolved spectroscopy of pyroxene on the surface, *Icarus*, *134*, 207–212, 1998.

Cruikshank, D. P., D. J. Tholen, W. K. Hartmann, J. F. Bell, and R. H. Brown, Three basaltic Earth-approaching asteroids and the source of basaltic meteorites, *Icarus*, *89*, 1–13, 1991.

Davoli, I., E. Paris, A. Mottana, and A. Marcelli, Xanes analysis on pyroxenes with different Ca concentration in M2 site, *Phys. Chem. Miner.*, *14*, 21–25, 1987.

Dodd, R. T., *Meteorites: A Chemical-Petrologic Synthesis*, Cambridge Univ. Press, New York, 1981.

Feierberg, M. A., H. P. Larson, U. Fink, and H. A. Smith, Spectroscopic evidence for 2 achondrite parent bodies: Asteroids 349 Dembowska and 4 Vesta, *Geochim. Cosmochim. Acta*, *44*, 513–524, 1980.

Gaffey, M. J., Spectral reflectance characteristics of the meteorite classes, *J. Geophys. Res.*, *81*, 905–920, 1976.

Gaffey, M. J., J. F. Bell, R. H. Brown, T. H. Burbine, J. L. Piatek, K. L. Reed, and D. A. Chaky, Mineralogical variations within the S-type asteroid class, *Icarus*, *106*, 573–602, 1993.

Ghose, S., Mg^{2+}-Fe^{2+} order in an orthopyroxene $Mg_{093}Fe_{107}Si_2O_6$, *Z. Kristallogr.*, *122*, 81–99, 1965.

Ghose, S., M. Kersten, K. Langer, G. Rossi, and L. Ungaretti, Crystal field spectra and Jahn Teller effect of Mn^{3+} in clinopyroxene and clinoamphiboles from India, *Phys. Chem. Miner.*, *13*, 291–305, 1986.

Goldman, D. S., and G. R. Rossman, Determination of quantitative cation distribution in orthopyroxenes from electronic absorption spectra, *Phys. Chem. Miner.*, *4*, 43–53, 1979.

Hazen, R. M., P. M. Bell, and H. K. Mao, Effects of compositional variation on absorption spectra of lunar pyroxenes, *Proc. Lunar Sci. Conf*, *9th*, 2919–2934, 1978.

Hillebrand, W. F., and G. E. F. Lundell, *Applied Inorganic Analysis with Special Reference to the Analysis of Metals, Minerals, and Rocks*, 2nd ed., revised by G. E. F. Lundell, H. A. Bright, and J. I. Hoffman, John Wiley, New York, 1953.

Hiroi, T., F. Vilas, and J. M. Sunshine, Discovery and analysis of minor absorption bands in S-asteroid visible reflectance spectra, *Icarus*, *119*, 202–208, 1996.

Howie, R. A., and J. V. Smith, X-ray emission microanalysis of rock-forming minerals: V. Orthopyroxenes, *J. Geol.*, *74*, 443–462, 1966.

Huguenin, R. L., The silicate component of Martian dust, *Icarus*, *70*, 162–188, 1987.

Hunt, G. R., and J. W. Salisbury, Visible and near-infrared spectra of minerals and rocks, I, Silicate minerals, *Mod. Geol.*, *1*, 283–300, 1970.

Ikeda, K., and K. Yagi, Experimental study on the phase equilibria in the join $CaMgSi_2O_6$ - $CaCrCrSiO_6$ with special reference to the blue diopsides, *Contrib. Mineral. Petrol.*, *61*, 91–106, 1977.

Ikeda, K., and K. Yagi, Crystal field spectra for blue and green diopsides synthesized in the join $CaMgSi_2O_6$ - $CaCrAlSiO_6$, *Contrib. Mineral. Petrol.*, *81*, 113–118, 1982.

Khomenko, V. M., and A. N. Platonov, Electronic absorption spectra of Cr^{3+} ions in natural clinopyroxenes, *Phys. Chem. Minerals*, *11*, 261–265, 1985.

Langer, K., and R. M. Abu-Eid, Measurement of the polarized absorption spectra of synthetic transition metal-bearing silicate microcrystals in the spectral range 44,000–4,000 cm^{-1}, *Phys. Chem. Miner.*, *1*, 273–299, 1977.

Mao, H. K., P. M. Bell, and J. S. Dickey, Comparison of the crystal-field spectra of natural and synthetic chrome diopside, *Year Book Carnegie Inst. Washington*, *71*, 538–541, 1972.

Mattson, S. M., and G. R. Rossman, Fe^{2+}-Ti^{4+} charge transfer in stoichiometric Fe^{2+}, Ti^{4+} minerals, *Phys. Chem. Miner.*, *16*, 78–82, 1988.

McCord, T. B., and R. N. Clark, The Mercury soil: Presence of Fe^{2+}, *J. Geophys. Res.*, *84*, 7664–7668, 1979.

McCord, T. B., J. B. Adams, and T. V. Johnson, Asteroid Vesta: Spectral reflectivity and compositional implications, *Science*, *168*, 1445–1447, 1970.

McFadden, L. A., M. J. Gaffey, H. Takeda, T. L. Jackowski, and K. L. Reed, Reflectance spectroscopy of diogenite meteorite types from Antarctica and their relationship to asteroids, *Mem. Natl. Inst. Polar Res., Spec. Iss.*, *25*, 188–206, 1982.

Molin, G. M., Crystal-chemical study of cation disordering in Al-rich and

Al-poor orthopyroxenes from spinel lherzolite xenoliths, *Am. Mineral.*, *74*, 593–598, 1989.

Neuhaus, A., Uber die Ionenfarben der Kristalle und Minerale am Beispiel der Chrommfarbungen, *Z. Kristallogr.*, *113*, 195–233, 1960.

Pieters, C. M., Strength of mineral absorption features in the transmitted component of near-infrared light: First results from RELAB, *J. Geophys. Res.*, *88*, 9534–9544, 1983.

RELAB, *Reflectance Experiment Laboratory (RELAB) Description and User's Manual*, Brown Univ., Providence, R. I., 1996.

Ross, N. L., and J. R. Sowerby, 1996. Crystal field spectrum of synthetic clinoferrosilite, in *Mineral Spectroscopy: A Tribute to Roger G. Burns*, edited by M. D. Dyar et al., pp. 273–280, Geochem. Soc., London, 1996.

Rossman, G. R., Pyroxene spectroscopy, in *Reviews in Mineralogy*, *vol. 7*, *Pyroxenes*, edited by C. T. Prewitt, pp. 93–116, Mineral. Soc. of Am., Washington, D. C., 1980.

Roush, T. L., Effects of temperature on remotely sensed mafic mineral absorption features, M.S. thesis, Univ. of Hawaii, Honolulu, 1984.

Runciman, W. A., D. Sengupta, and M. Marshall, The polarized spectra of iron in silicates, I, Enstatite, *Am. Mineral.*, *58*, 444–450, 1973.

Schmetzer, K., Absorption spectroscopy and colour of V^{3+}-bearing natural oxides and silicates - a contribution to the crystal chemistry of vanadium, *Neues Jahrb. Mineral. Abh.*, *144*, 73–126, 1982.

Schreiber, H. D., On the nature of synthetic blue diopside crystals: The stabilization of tetravalent chromium, *Am. Mineral.*, *62*, 522–527, 1977.

Schreiber, H. D., Chromium, blue diopside, and experimental petrology, a discussion, *Contrib. Mineral. Petrol.*, *66*, 341–342, 1978.

Sherman, D. M., Molecular orbital (SCF-Xα-SW) theory of metal-metal charge transfer processes in minerals, II, Application to Fe^{2+} |Ti^{4+} charge transfer transitions in oxides and silicates, *Phys. Chem. Miner.*, *14*, 364–367, 1987.

Singer, R. B., J. S. Miller, K. W. Wells, and E. S. Bus, Visible and near-IR spectral imaging of Mars during the 1988 opposition (abstract), *Lunar Planet. Sci.*, *21*, 1164–1165, 1990.

Steffen, G., K. Langer, and F. Seifert, Polarized electronic absorption spectra of synthetic (Mg-Fe)-orthopyroxenes, ferrosilite and Fe^{3+}-bearing ferrosilite, *Phys. Chem. Miner.*, *16*, 120–129, 1988.

Sunshine, J. M., and C. M. Pieters, Estimating modal abundances from the spectra of natural and laboratory pyroxene mixtures using the modified Gaussian model, *J. Geophys. Res.*, *98*, 9075–9087, 1993.

Surkov, Y. A., L. P. Moskalyeva, O. P. Shcheglov, V. P. Kharyukovo, O. S. Manvelyan, V. S. Kirichenko, and A. D. Dudin, Determination of the elemental composition of rocks on Venus by Venera 13 and Venera 14 (Preliminary results), *Proc. Lunar Planet. Sci. Conf. 13th*, Part 1, *J. Geophys. Res.*, *88*, suppl., A481–A492, 1983.

Tazzoli, V., and M. C. Domeneghetti, Crystal-chemistry of natural and heated aluminous orthopyroxenes, *Phys. Chem. Minerals*, *15*, 131–139, 1987.

Warren, B. E., and W. L. Bragg, The structure of diopside $CaMg(SiO_3)_2$, *Z. Kristallogr.*, *69*, 168–193, 1929.

Weidner, V. R., and J. J. Hsia, Reflection properties of pressed polytetrafluoroethylene powder, *J. Opt. Soc. Am.*, *71*, 856–861, 1981.

White, W. B., and K. L. Keester, Optical absorption spectra of iron in the rock forming silicates, *Am. Mineral.*, *51*, 774–791, 1966.

White, W. B., G. J. McCarthy, and B. E. Scheetz, Optical spectra of chromium, nickel, and cobalt-containing pyroxenes, *Am. Miner.*, *56*, 72–89, 1971.

Wood, C. A., and L. D. Ashwal, SNC meteorites: Igneous rocks from Mars?, *Proc. Lunar Planet. Sci. Conf.*, *12*, 1359–1375, 1981.

Zhao, S.-B., H.-S. Wang, K.-W. Zhou, and T.-B. Xiao, The spin-forbidden absorption spectrum of Fe^{2+} in orthopyroxene, *Phys. Chem. Miner.*, *13*, 96–101, 1986.

E. A. Cloutis, Department of Geography, University of Winnipeg, 515 Portage Avenue, Winnipeg, Manitoba, Canada R3B 2E9. (e.cloutis@uwinnipeg.ca)